Eukaryotic Cell

Members of the Penicillium chrysogenum Velvet Complex Play Functionally Opposing Roles in the Regulation of Penicillin Biosynthesis and Conidiation

Katarina Kopke, Birgit Hoff, Sandra Bloemendal, Alexandra Katschorowski, Jens Kamerewerd and Ulrich Kück

Eukaryotic Cell **2013, 12(2):299. DOI: 10.1128/EC.00272-12. Published Ahead of Print 21 December 2012.**

EC
Journals.ASM.org

Members of the *Penicillium chrysogenum* Velvet Complex Play Functionally Opposing Roles in the Regulation of Penicillin Biosynthesis and Conidiation

Katarina Kopke, Birgit Hoff,* Sandra Bloemendal, Alexandra Katschorowski, Jens Kamerewerd, Ulrich Kück

Christian Doppler Laboratory for Fungal Biotechnology, Lehrstuhl für Allgemeine und Molekulare Botanik, Ruhr-Universität Bochum, Bochum, Germany

A velvet multisubunit complex was recently detected in the filamentous fungus *Penicillium chrysogenum*, the major industrial producer of the β-lactam antibiotic penicillin. Core components of this complex are *P. chrysogenum* VelA (PcVelA) and PcLaeA, which regulate secondary metabolite production, hyphal morphology, conidiation, and pellet formation. Here we describe the characterization of PcVelB, PcVelC, and PcVosA as novel subunits of this velvet complex. Using yeast two-hybrid analysis and bimolecular fluorescence complementation (BiFC), we demonstrate that all velvet proteins are part of an interaction network. Functional analyses using single- and double-knockout strains clearly indicate that velvet subunits have opposing roles in the regulation of penicillin biosynthesis and light-dependent conidiation. PcVelC, together with PcVelA and PcLaeA, activates penicillin biosynthesis, while PcVelB represses this process. In contrast, PcVelB and PcVosA promote conidiation, while PcVelC has an inhibitory effect. Our genetic analyses further show that light-dependent spore formation depends not only on PcVelA but also on PcVelB and PcVosA. The results provided here contribute to our fundamental understanding of the function of velvet subunits as part of a regulatory network mediating signals responsible for morphology and secondary metabolism and will be instrumental in generating mutants with newly derived properties that are relevant to strain improvement programs.

The β-lactam antibiotic penicillin was discovered almost a century ago (1) and since then has been used to treat bacterial infections. With estimated yearly sales of about $8 billion, penicillin, along with cephalosporin C, is one of the most valued products in the global anti-infective market (2). Although other filamentous fungi such as *Aspergillus nidulans* are able to produce penicillin, a wild-type isolate of *Penicillium chrysogenum* is the exclusive source for carefully derived production strains used in industry to obtain economically relevant penicillin titers (3). In all penicillin-producing fungi, biosynthesis is catalyzed by three enzymes: δ-(L-α-aminoadipyl)-L-cysteinyl-D-valine synthetase (ACVS), isopenicillin N synthase (IPNS), and acyl-coenzyme A (acyl-CoA):isopenicillin N acyltransferase (IAT) (reviewed in reference 4). The corresponding genes *pcbAB* (syn. *acvA*), *pcbC* (syn. *ipnA*), and *penDE* (syn. *aatA*) are found in a single cluster that is structurally conserved in pro- and eukaryotic microbial producers (5–7).

Recent studies in filamentous fungi have shown that the regulation of many clustered genes and, thus, biosynthesis of secondary metabolites such as antibiotics are usually associated with cellular differentiation processes (7, 8). However, the regulatory networks connecting natural-product biosynthesis and fungal development in relation to environmental factors are highly complex and not currently completely understood at the genetic level.

A first advance in gaining greater insights into these networks was the discovery of a G-protein-mediated pathway in the fungus *A. nidulans* (9, 10). Since then, several studies have provided further profound insights into other factors that link production of secondary metabolites and morphological differentiation processes (11). In *Acremonium chrysogenum*, for example, two interacting transcription factors, CPCR1 and AcFKH1, regulate both cephalosporin C production and asexual arthrospore formation (12–14). An even more complex regulation network was observed recently, when the multisubunit velvet complex was shown to link both differentiation processes in *A. nidulans* (15–19). The founding member of this complex is velvet (VeA), discovered in a *veA* mutant, which was described more than 40 years ago (20) and is now eponymous for the velvet superfamily. Under dark conditions, this protein forms a heterotrimeric complex with VelB, another protein of the velvet family, and the global regulator of secondary metabolism LaeA (17, 21).

A third velvet protein, namely, VosA, also interacts in the dark with VelB, and it is proposed that this heterodimer can repress asexual spore formation as well as control spore maturation and trehalose biogenesis (22, 23). Shuffling of VelB between the VelB-VosA and VeA-LaeA complexes is controlled by the LaeA protein, which therefore plays a key dynamic role in regulating secondary metabolism and development in *A. nidulans* (23). In contrast, the function of VelC, the fourth member of the velvet superfamily, is still unclear (24). The velvet protein VeA and the other complex subunits are highly conserved in various fungi (25). However, despite their structural conservation, several studies have shown that the regulators possess marked functional plasticity in different species, thus reflecting the diversity of fungal lifestyles (19, 24).

Recently, we have described the VeA and LaeA homologs from *P. chrysogenum*, which interact with each other and regulate not

Received 28 September 2012 **Accepted** 12 December 2012

Published ahead of print 21 December 2012

Address correspondence to Ulrich Kück, ulrich.kueck@rub.de.

* Present address: Birgit Hoff, BASF SE, Ludwigshafen, Germany.

K.K., B.H., and S.B. contributed equally to this article.

Supplemental material for this article may be found at http://dx.doi.org/10.1128/EC.00272-12.

doi:10.1128/EC.00272-12

The authors have paid a fee to allow immediate free access to this article.

TABLE 1 *P. chrysogenum* strains used in this work

Strain	Relevant genotype	Reference or source
P2niaD18	Penicillin producer; *niaD*$^-$	31
BiFC-PcVelA/PcVelC	*Pgpd*::P*cvelA*::*eyfpN*::*TtrpC*; *Pgpd*::P*cvelC*::*eyfpC*::*TtrpC*; *PtrpC*::*nat1*; *niaD*$^-$	This study
BiFC-PcVelA/PcVosA	*Pgpd*::P*cvelA*::*eyfpN*::*TtrpC*; *Pgpd*::P*cvosA*::*eyfpC*::*TtrpC*; *PtrpC*::*nat1*; *niaD*$^-$	This study
BiFC-PcVelB/PcVosA	*Pgpd*::P*cvosA*::*eyfpN*::*TtrpC*; *Pgpd*::P*cvelB*::*eyfpC*::*TtrpC*; *PtrpC*::*nat1*; *niaD*$^-$	This study
BiFC-PcVelC/PcVosA	*Pgpd*::P*cvosA*::*eyfpN*::*TtrpC*; *Pgpd*::P*cvelC*::*eyfpC*::*TtrpC*; *PtrpC*::*nat1*; *niaD*$^-$	This study
Δ*Pcku70*^{b} (P*cku70FRT2*)	Δ*Pcku70*::*FRT*; *niaD*$^-$	32
Δ*Pcku70*^{c} (P2:KU70i)	*Pxyl*::P*cku70s*::P*cku70as*::*TtrpC*, *ptrA(p)*::*ptrA*	33
Δ*PcvelA*^{a}	Δ*Pcku70*::*FRT*; Δ*PcvelA*::*FRT*::*Pxyl*::P*cflp*::*PtrpC*::*nat1*::*FRT*; *niaD*$^-$	This study
Δ*PcvelA*^{b}	Δ*Pcku70*::*FRT*; Δ*PcVelA*::*FRT*; *niaD*$^-$	This study
Δ*PcvelB*^{a}	Δ*Pcku70*::*FRT*; Δ*PcvelB*::*FRT*::*Pxyl*::P*cflp*::*PtrpC*::*ble*::*FRT*; *niaD*$^-$	K. Kopke and U. Kück, unpublished data
Δ*PcvelB*^{b}	Δ*Pcku70*::*FRT*; Δ*PcvelB*::*FRT*; *niaD*$^-$	Kopke and Kück, unpublished
Δ*PcvelC*^{a}	Δ*Pcku70*::*FRT*; Δ*PcvelC*::*FRT*::*Pxyl*::P*cflp*::*PtrpC*::*nat1*::*FRT*; *niaD*$^-$	This study
Δ*PcvelC*^{b}	Δ*Pcku70*::*FRT*; Δ*PcvelC*::*FRT*; *niaD*$^-$	This study
Δ*PcvosA*	Δ*Pcku70*::*FRT*; Δ*PcvosA*::*PtrpC*::*nat1*; *niaD*$^-$	This study
Δ*PclaeA*^{c} (P2:KU70i:Δ*PclaeA*)	*Pxyl*::P*cku70s*::P*cku70as*::*TtrpC*, *ptrA(p)*::*ptrA*; Δ*PclaeA*::*PtrpC*::*ble*	33
Δ*PcvelC*^{b}::P*cvelC*	Δ*Pcku70*::*FRT*; Δ*PcvelC*::*FRT*; *Pgpd*::P*cvelC*::*eyfpN*::*TtrpC*; *PtrpC*::*nat1*; *niaD*$^-$	This study
Δ*PcvelB*^{b}::P*cvelB*	Δ*Pcku70*::*FRT*; Δ*PcvelB*::*FRT*::*PtrpC*::*ble*::*PtrpC*::P*cvelB*::*FRT*; *niaD*$^-$	Kopke and Kück, unpublished
Δ*PcvelA*Δ*PcvelB*^{a}	Δ*Pcku70*::*FRT*; Δ*PcvelB*::*FRT*; Δ*PcvelA*::*FRT*::*Pxyl*::P*cflp*::*PtrpC*::*nat1*::*FRT*; *niaD*$^-$	This study
Δ*PcvelA*Δ*PcvelC*^{a}	Δ*Pcku70*::*FRT*; Δ*PcvelC*::*FRT*; Δ*PcvelA*::*FRT*::*Pxyl*::P*cflp*::*PtrpC*::*nat1*::*FRT*; *niaD*$^-$	This study
Δ*PcvelA*Δ*PcvelC*^{b}	Δ*Pcku70*::*FRT*; Δ*PcvelA*::*FRT*; Δ*PcvelC*::*FRT*; *niaD*$^-$	This study
Δ*PcvelB*Δ*PcvelC*^{a}	Δ*Pcku70*::*FRT*; Δ*PcvelC*::*FRT*; Δ*PcvelB*::*FRT*::*Pxyl*::P*cflp*::*PtrpC*::*ble*::*FRT*; *niaD*$^-$	This study
Δ*PcvelB*Δ*PcvosA*^{a}	Δ*Pcku70*::*FRT*; Δ*PcvosA*::*PtrpC*::*nat1*; Δ*PcvelB*::*FRT*::*Pxyl*::P*cflp*::*PtrpC*::*ble*::*FRT*; *niaD*$^-$	This study
Δ*PclaeA*Δ*PcvelA*^{c} (P2:KU70i:Δ*PclaeA*:Δ*PcvelA*)	*Pxyl*::P*cku70s*::P*cku70as*::*TtrpC*, *PptrA*::*ptrA*; Δ*PclaeA*::*PtrpC*::*ble*; Δ*PcvelA*::*PtrpC*::*nat1*	33

[a] Strains still carrying resistance marker from the flipper knockout construct.
[b] Strains without any resistance markers due to FLP/*FRT* marker recycling.
[c] Strains generated by using RNA interference.

only penicillin biosynthesis but also hyphal morphology, conidiation, and pellet formation (26). However, the underlying molecular mechanisms of how these components control the biochemical and morphological differentiation processes are still poorly understood; without a thorough understanding of the determinants regulating secondary metabolism and morphogenesis, the genetic manipulation of fungal metabolisms as part of industrial strain improvement programs is rendered difficult.

Here we conducted a detailed genetic study using single- and double-knockout mutants to unravel the function of the newly discovered velvet superfamily members *P. chrysogenum* VelB (PcVelB), PcVelC, and PcVosA during development of *P. chrysogenum*. Interaction studies together with bioassays and sporulation analyses determined that these three proteins are part of the velvet complex in *P. chrysogenum* and, in some cases, are essential for proper penicillin production and conidiation. Moreover, our genetic data indicate opposing roles for distinct subunits in morphogenesis and secondary metabolism. Our report also provides a detailed analysis of PcVelC, for which homologs have not yet been functionally characterized. Furthermore, the generation of multiple knockout strains substantially extends our fundamental understanding of the underlying molecular mechanisms involved in the regulatory role of the fungal velvet complex.

MATERIALS AND METHODS

Strains and culture conditions. Recombinant plasmids were generated using either standard laboratory techniques (27) or an In-fusion Advantage PCR cloning kit (Clontech) following the manufacturer's instructions with *Escherichia coli* strain XL1-Blue MRF′ as host for general plasmid construction and maintenance (28) or by homologous recombination in *Saccharomyces cerevisiae* strain PJ69-4A as described previously (29). Yeast cells were transformed in a Multiporator (Eppendorf, Germany) at 1.5 kV by electroporation according to the method of Becker and Lundblad (30).

All *P. chrysogenum* strains used in this study are listed in Table 1. P2niaD18 (34) is the parental strain of the marker-free Δ*Pcku70* strain and was previously derived from the sequenced strain Wisconsin 54-1255 (35). The marker-free Δ*Pcku70* strain served as a recipient for the construction of knockout mutants (32). In addition to newly generated deletion strains, the recently described Δ*PclaeA* and Δ*PclaeA* Δ*PcvelA* strains were used for functional characterization (33). All *P. chrysogenum* strains were grown either in liquid complex medium (CCM) or minimal medium (MM) at 27°C and 120 rpm or on solid medium as already described (33). For induction of the *P. chrysogenum* Pcflp-mediated site-specific recombination, appropriate strains were grown on solid MM supplemented with 2% xylose (32, 36). To inoculate shake flasks and solid medium, we used spores collected from 7-day-old cultures grown on medium M322. Transformation of individual *P. chrysogenum* strains was performed as described previously (33, 34), and transformants were selected by growth on solid medium supplemented with 200 μg ml^{-1} nourseothricin, 40 μg ml^{-1} phleomycin, or 700 μg ml^{-1} pyrithiamine.

Construction of plasmids. All plasmids and oligonucleotides used in this work are given in Table 2 and Table S1 in the supplemental material, respectively. The 5′- and 3′-flanking regions of P*cvelA* were amplified from genomic DNA by PCR to construct a P*cvelA*-specific *nat1* flipper cassette for P*cvelA* gene deletion. Primer pair P1 and P2 was used for amplification of the 5′-flanking region containing linker for Bst1107I and NdeI endonucleases, resulting in an amplicon of 1.1 kb. The 1.1-kb 3′-

TABLE 2 Plasmids used in this work

Plasmid	Characteristic(s)	Reference or source
pDrive	UA-based PCR cloning	Qiagen
pDNAT-FRT1-2	5′ *FRT* sequence, *trpC* promoter of *A. nidulans*, *nat1* gene of *Streptomyces noursei*, 3′ *FRT* sequence	32
pLarge	5′ *FRT* sequence, *xyl* promoter *of P. chrysogenum*, codon-adapted Pc*flp* recombinase gene, *trpC* promoter of *A. nidulans*, *nat1* resistance gene of *S. noursei*, 3′ *FRT* sequence	This study
pKAvelA-Flip	5′ Pc*velA* fragment, 5′ *FRT* sequence, *xyl* promoter *of P chrysogenum*, codon-adapted Pc*flp* recombinase gene, *trpC* promoter of *A. nidulans*, *nat1* resistance gene of *S. noursei*, 3′ *FRT* sequence, 3′ Pc*velA* fragment	This study
p3′velC	5′ *FRT* sequence, *xyl* promoter *of P. chrysogenum*, codon-adapted Pc*flp* recombinase gene, *trpC* promoter of *A. nidulans*, *nat1* resistance gene of *S. noursei*, 3′ *FRT* sequence, 3′ Pc*velC* fragment	This study
pKAvelC-Flip	5′ Pc*velC* fragment, 5′ *FRT* sequence, *xyl* promoter *of P. chrysogenum*, codon-adapted Pc*flp* recombinase gene, *trpC* promoter of *A. nidulans*, *nat1* resistance gene of *S. noursei*, 3′ *FRT* sequence, 3′ Pc*velC* fragment	This study
pKOvelB-Flip	5′ Pc*velB* fragment, 5′ *FRT* sequence, *xyl* promoter *of P. chrysogenum*, codon-adapted Pc*flp* recombinase gene, *trpC* promoter of *A. nidulans*, *ble* resistance gene of *Streptoalloteichus hindustanus*, 3′ *FRT* sequence, 3′ Pc*velB* fragment	Kopke and Kück, unpublished
pRS426	*ura3(p)*::*URA3*	37
pKOvosA	5′ Pc*vosA* fragment, *trpC* promoter of *A. nidulans*, *nat1* resistance gene of *S. noursei*, 3′ Pc*vosA* fragment	This study
pGADT7	*ADH1(p)*::*gal4 AD*::*LEU2*	Clontech
pGBKT7	*ADH1(p)*::*gal4 BD*::*TRP1*	Clontech
pAD-PcvelA	Pc*velA* cDNA in SmaI and SacI site in pGADT7	This study
pAD-PcvelB	Pc*velB* cDNA in NcoI site in pGADT7	This study
pAD-PcvelC	Pc*velC* cDNA in EcoRI and BamHI site in pGADT7	This study
pAD-PcvosA	Pc*vosA* cDNA in EcoRI and XhoI site in pGADT7	This study
pAD-PclaeA	Pc*laeA* cDNA in EcoRI and XhoI site in pGADT7	This study
pBD-PcvelA	Pc*velA* cDNA in SmaI and SacI site in pGBKT7	This study
pBD-PcvelB	Pc*velB* cDNA in NcoI site in pGBKT7	This study
pBD-PcvelC	Pc*velC* cDNA in EcoRI and BamHI site in pGBKT7	This study
pBD-PcvosA	Pc*vosA* cDNA in EcoRI and XhoI site in pGBKT7	This study
pBD-PclaeA	Pc*laeA* cDNA in EcoRI and PstI site in pGBKT7	This study
pEYFPC-nat	*gpd* promoter of *A. nidulans*, $eyfp_C$ fragment (aa 155–238), *trpC* terminator of *A. nidulans*, *nat1* gene	26
pEYFPN-nat	*gpd* promoter of *A. nidulans*, $eyfp_N$ fragment (aa 1–154), *trpC* terminator of *A. nidulans*, *nat1* gene	26
pYNVELA	Pc*velA* ORF in NotI site of pEYFPN-nat	26
pYCVELB	Pc*velB* ORF in NotI site of pEYFPC-nat	26
pYNVELC	Pc*velC* ORF in NcoI site of pEYFPN-nat	This study
pYCVOSA	Pc*vosA* ORF in NotI site of pEYFPC-nat	This study
pYNVOSA	Pc*vosA* ORF in NotI site of pEYFPN-nat	This study

flanking region of Pc*velA* was amplified with oligonucleotides P3 and P4. Both PCR fragments were subcloned in pDrive (Qiagen, Germany) and sequenced. Subsequently, both flanking sequences were cloned into pDNAT1-FRT1-2 (32) using an In-fusion Advantage PCR cloning kit (Clontech). In a final step, the *xyl(p)*-Pc*flp* fragment, isolated from plasmid pLarge, completed the Pc*velA*-specific flipper cassette, resulting in plasmid pKAvelA-Flip. For transformation in *P. chrysogenum*, the 6.4-kb Pc*velA*-specific *nat1* flipper was isolated through restriction with Bst1107I and HpaI. The Pc*velC*-specific flipper cassette was constructed similarly to the Pc*velA* flipper, with the exception that Bst1107I and SwaI were used as flanking restriction sites. In this experiment, primer pair P5 and P6 and primer pair P7 and P8 were used for amplification of the 5′- and 3′-flanking sequences of Pc*velC*. To construct a Pc*velCFL*-specific *nat1* flipper for Pc*velC* gene deletion, 1.4 kb of the 5′-flanking region of Pc*velC* was amplified with primers P9 and P10 and inserted into NotI-HpaI-digested plasmid p3′velC, resulting in plasmid pKAvelC-Flip. For transformation in *P. chrysogenum*, the 6.7-kb Pc*velC*-specific *nat1* flipper was isolated by restriction with Bst1107I and HpaI. The generation of plasmid pKOvelB-Flip is described elsewhere (K. Kopke and U. Kück, unpublished data).

To delete the Pc*vosA* gene, plasmid pKOvosA was generated by homologous recombination in *S. cerevisiae* strain PJ69-4A. For this purpose, the 5′- and 3′-flanking regions of Pc*vosA* as well as the *nat1* resistance marker controlled by the *trpC* promoter of *A. nidulans* were amplified by PCR using primer pair P13 and P14, primer pair P15 and P16, and primer pair P17 and P18, respectively. In a final step, the three amplicons and the XhoI-EcoRI-hydrolyzed plasmid pRS426 were assembled in yeast using the endogenous homologous recombination system. The resulting plasmid was named pKOvosA and carried the complete Pc*vosA* deletion cassette.

To construct the Pc*velA* two-hybrid plasmids, the cDNA of the entire coding region of Pc*velA* was amplified with primers P42 and P43 and inserted into SmaI-SacI-digested vector pGADT7 (Clontech) containing the Gal4 activation domain (AD), resulting in plasmid pAD-PcvelA. To generate pBD-PcvelA, plasmid pAD-PcvelA was hydrolyzed with PvuI as well as NcoI and a 0.8-kb fragment of Pc*velA* was used for further homologous recombination in yeast. Using primer pair P44 and P45 and primer pair P46 and P47, fragments of 0.5 kb and 0.6 kb encoding the N-terminal and C-terminal parts of Pc*velA*, respectively, were amplified. All three fragments and the linearized vector pGBKT7 (Clontech), containing the Gal4 DNA binding domain (BD), were transformed into *S. cerevisiae* for homologous recombination as described above. Transformants were selected for tryptophan prototrophy. To generate two-hybrid plasmid pAD-PcvelB carrying the complete Pc*velB* open reading frame (ORF), the cDNA of Pc*velB*, amplified with oligonucleotides P48 and P49, was inserted into EcoRI-BamHI-digested pGADT7. Plasmid pBD-PcvelB was obtained after excision of Pc*velB* from pAD-PcvelB with EcoRI and BamHI and ligation into vector pGBKT7. To generate the Pc*velC* two-hybrid plasmids, the cDNA of the entire coding region of Pc*velC* was amplified with oligonucleotides P50 and P51 and inserted into EcoRI-BamHI-digested pGADT7 and pGBKT7, resulting in plasmids pAD-

PcvelC and pBD-PcvelC, respectively. For construction of the P*cvosA* two-hybrid plasmids, a cDNA fragment encoding the full-length protein was amplified with primer pair P52 and P53 and cloned into EcoRI-XhoI-digested pGBKT7, resulting in plasmid pBD-PcvosA. P*cvosA* was then excised from pBD-PcvosA with EcoRI and XhoI and ligated into vector pGADT7 to generate plasmid pAD-PcvosA. To generate pAD-PclaeA, a 0.4-kb fragment of P*claeA* coding for the N-terminal part was amplified from cDNA using primer pair P54 and P55. With primers P56 and P57, a 0.9-kb fragment coding for the C-terminal part of P*claeA* was amplified from genomic DNA. Both fragments and the EcoRI-XhoI-linearized vector pGADT7 were transformed into *S. cerevisiae* for homologous recombination. Transformants were selected for leucine prototrophy. To construct plasmid pBD-PclaeA, a 0.4-kb fragment of P*claeA* coding for the N-terminal part was amplified from cDNA with primers P55 and P58. Using primer pair P56 and P59, a 0.9-kb fragment coding for the C-terminal part of P*claeA* was amplified from genomic DNA. Both fragments and the EcoRI-PstI-linearized vector pGBKT7 were transformed into *S. cerevisiae* for homologous recombination. Transformants were selected for tryptophan prototrophy.

To construct plasmids for bimolecular fluorescence complementation (BiFC) (13), P*cvosA* was amplified by PCR with primer pair P60 and P61 and subsequently ligated into the NotI site of pEYFPC-nat and pEYFPN-nat, resulting in plasmids pYCVOSA and pYNVOSA, respectively. To generate vector pYNVELC, the sequence encoding the open reading frame of P*cvelC* was amplified by PCR using primers P11 and P12 to introduce NcoI sites. After subcloning, the NcoI fragment was ligated into the corresponding site of pEYFPN-nat, resulting in plasmid pYNVELC.

Construction of knockout mutants and complementation strains. All oligonucleotides used for verification of knockout strains are given in Table S1 in the supplemental material. Single knockout strains for P*cvelA*, P*cvelC*, and P*cvosA* were constructed using the ΔP*cku70* strain (32). For this purpose, gene-specific *nat1* flippers were used to replace P*cvelA* or P*cvelC* by homologous integration. The ΔP*cvosA* mutant was generated by using a conventional knockout cassette, which consisted of the *nat1* resistance gene and the 5′ and 3′ flanking regions of P*cvosA*. For P*cvelC*, a knockout was constructed to delete a part of the 3′ region of the gene encoding the 290 amino acids (aa) of the C-terminal of the polypeptide. This region covers the conserved velvet domain as well as sequences for putative nuclear localization signals (NLSs) and nuclear export sequences (NESs).

In the following, we describe in detail the strategy for the construction of the marker-free P*cvelA* knockout, which was applied identically for the ΔP*cvelC* strain. After transformation of the P*cvelA*-specific *nat1* flipper, the resulting transformants were verified by PCR. Primer sets generated an amplicon of either 1.3 kb (P27/P35) or 1.4 kb (P28/P35), thus confirming the homologous integration of the P*cvelA*-specific *nat1* flipper at the P*cvelA* locus. Using primers P19 and P20, no amplification of the P*cvelA* gene was observed in single spore isolates, while the ΔP*cku70* strain served as a positive control. Next, the excision of the *nat1* flipper was performed by xylose-induced P*cflp* gene expression. Strains were grown for 12 to 18 days on solid MM containing 2% xylose as a single carbon source. Pcflp-mediated excision was detected by growth tests on selection medium and verified by PCR. By generating a 2.6-kb fragment using primer pair P27 and P28, a Pcflp-mediated site-specific recombination event was identified. Subsequently, single-spore isolate T5.13 was further analyzed by Southern hybridization using the 1.2-kb 3′-P*cvelA* flank as a probe. As expected, a 2.9-kb fragment of NcoI-digested genomic DNA of the knockout strain was detected on the autoradiogram, while the recipient ΔP*cku70* strain rendered a 2.6-kb fragment, which is indicative for the native P*cvelA* locus.

The ΔP*cvelB* mutant was generated by using a P*cvelB*-specific *ble*-Flipper construct (Kopke and Kück, unpublished).

For rescue of the disruption strains, complementation assays were performed. Plasmid pYNVELC was ectopically integrated to restore the P*cvelC* phenotype of the marker-free ΔP*cvelC* strain.

To generate multiple-deletion strains, the codon-adapted FLP/*FRT* recombination system was used for efficient marker recycling. Four double-knockout strains, the ΔP*cvelA* ΔP*cvelB*, ΔP*cvelA* ΔP*cvelC*, ΔP*cvelB* ΔP*cvelC*, and ΔP*cvelB* ΔP*cvosA* strains, were constructed by homologous integration of a second flipper cassette. The ΔP*cvelB* strain was used for the generation of the double-knockout ΔP*cvelA* ΔP*cvelB* mutant, whereas the marker-free knockout ΔP*cvelC* strain served as recipient for additional deletion of P*cvelA* or P*cvelB*. In addition, the ΔP*cvosA* strain was used to construct the ΔP*cvelB* ΔP*cvosA* strain. These further deletions of P*cvelA* and P*cvelB* were verified by PCR analysis as already described for the single-knockout strains. A summary of all mutants generated in this investigation is provided in Table 1, and the strategy of knockout construction as well as the genealogy of strains is given in Fig. S1 and S2 in the supplemental material.

Nucleic acid preparations and manipulations. Isolation of fungal genomic DNA and RNA was carried out as described previously (38, 39), and DNA or RNA was isolated from hyphal cells grown at 27°C and 120 rpm for 72 h in liquid media. Southern blotting was performed with GeneScreen hybridization transfer membrane (PerkinElmer) and hybridized with [α-^{32}P]dCTP-labeled probes using standard methods (27), and cDNA synthesis was done as previously described (31).

Yeast two-hybrid assay. The prey and bait plasmids were constructed as described in the "Construction of plasmids" section, confirmed by sequencing, and transformed into *S. cerevisiae* strains Y187 (Clontech) for BD fusion derivates and AH109 (Clontech) for AD fusion derivates. Yeast two-hybrid experiments were performed according to Bloemendal et al. (40) with minor modifications. After mating, diploids were selected on minimal medium for leucine and tryptophan prototrophy. Diploids containing both two-hybrid vectors were screened for activity of the reporter genes *HIS3*, *ADE2*, and *lacZ*. Analysis of reporter gene expression was carried out by transferring diploids onto media with X-α-galactosidase (X-α-Gal), but without adenine and histidine.

Quantification of conidiation. To measure conidiation of the reference strain, the knockout mutants and complementation strains were grown on solid M322 medium to obtain spore suspensions with a concentration of 1×10^7 spores/ml. Solid minimal medium with glucose was inoculated with 10 μl or 200 μl of the spore suspensions, depending on whether phenotypic or quantitative assays were conducted. Incubation under light or dark conditions was performed for 168 h at 27°C. For quantitative assays, a disc with a diameter of 1 cm was cut out of the plate and transferred to a Falcon tube with 10 ml suspension buffer (0.85% [wt/vol] NaCl, 0.1% [wt/vol] Tween). The samples were then boiled for 30 min. To separate spores, each sample was treated with a sonifier (Sonifier 250; Brandson) for 5 min and appropriate dilutions were made to determine the spore concentration with an Abbe-Zeiss counting cell chamber. All spore measurements were performed in triplicate, from at least two independent isolates.

Spore viability assay. Strains were grown for 4, 7, 10, and 13 days on solid complete M322 medium to obtain spore suspensions with a concentration of 1×10^7 spores/ml. Approximately 100 conidia were inoculated on complete medium (M322), and after 4 days of incubation at 27°C, germinating spores were counted. All measurements were performed in triplicate from at least two independent isolates.

Penicillin bioassay. For a penicillin bioassay, 50 ml of CCM was inoculated with 5×10^6 spores. Cultures were incubated for 72, 96, 120, and 144 h at 27°C and 120 rpm. After harvesting, supernatants were used to perform the penicillin bioassay, with *Staphylococcus aureus* as the indicator organism. The obtained mycelia were used to measure the dry weight. All experiments were performed in triplicate from at least two independent isolates. For penicillinase assays, supernatants were incubated with penicillinase from *Bacillus cereus* (Sigma-Aldrich, St. Louis, MO) according to the manufacturer's instructions.

Microscopy. Microscopy for BiFC was performed as described before (26) with minor modifications. For imaging, Metamorph (version 7.7.5.0;

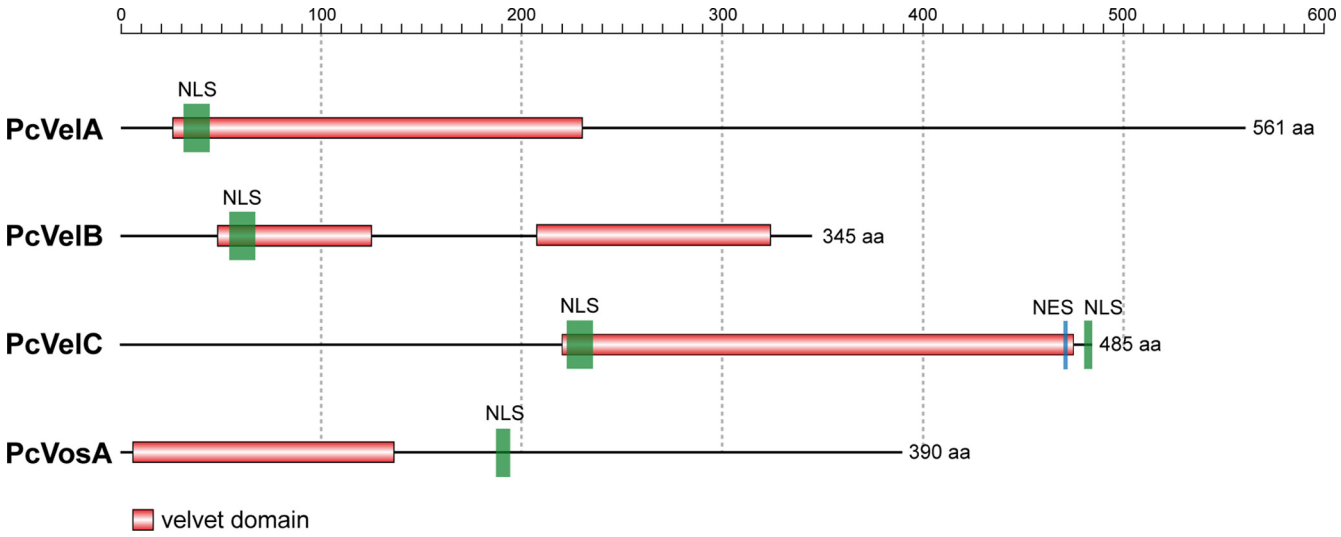

FIG 1 Comparison of velvet proteins from *P. chrysogenum*. The predicted protein structures of velvet components PcVelA, PcVelB, PcVelC, and PcVosA are given. All four proteins possess a conserved velvet domain (red) as well as predicted nuclear localization signals (NLS, green). For PcVelC, a putative nuclear export sequence (NES) is shown in blue.

Universal Imaging) was used and recorded images were processed with MetaMorph and Adobe Photoshop CS4.

Computational biology. NLSs and NESs were predicted with WoLF PSORT (41) and NetNES 1.1 (42), respectively. Protein sequence alignments were performed using the CLUSTALW program (43). Sequences representing conserved motifs were manually extracted from alignments edited with GeneDoc (44). Microarray analysis was performed as described previously by Hoff et al. (26). The microarray data used in this study are available from the GSE18585 series at the NCBI Gene Expression Omnibus (GEO) repository (26, 45).

RESULTS

Sequence comparison of velvet proteins from *Penicillium chrysogenum*. We have recently described PcVelA, a core component of the velvet complex, which is associated with PcLaeA, a regulator of secondary metabolism in *P. chrysogenum* (26). The PcVelA sequence from *P. chrysogenum* together with sequences homologous to velvet subunits from different *Aspergilli* and *Neosartoria* species served as sources to identify genes encoding velvet proteins PcVelB, PcVelC, and PcVosA in the *P. chrysogenum* genome (35). Analysis of multiple protein alignments, including alignment of PcVelA, revealed a conserved amino acid motif with high sequence similarity to the velvet domain described recently for *A. nidulans* velvet components (Fig. 1; see also Fig. S3 and Table S2 in the supplemental material) (24, 25). In contrast to PcVelA and PcVosA, where the velvet domain is located close to the N terminus, this motif is located in the C-terminal part of PcVelC (Fig. 1). In PcVelB, the velvet domain is split into two parts with one in the N terminus and the other one in the C terminus of the protein (Fig. 1). In three out of four subunits (PcVelA, PcVelB, and PcVelC), we detected a nuclear localization signal (NLS) (46) within the velvet domain, and using the program WoLF PSORTII, we found two further NLSs, one at the C terminus of PcVelC and another one centrically within the main body of PcVosA. In addition, a predicted nuclear export sequence (NES) was detected at the C terminus of PcVelC (Fig. 1).

We analyzed the P*cvelC* transcript to localize the most likely start codon within the P*cvelC* mRNA. Analysis of the sequences of cDNA clones revealed a start codon more than 1 kb upstream of the previously predicted translational start, a finding that indicates that the coding region of P*cvelC* is longer than that initially proposed by van den Berg et al. (35). Moreover, this N-terminal region comprises no putative conserved domains and comparison with different aspergilli revealed that this part is highly variable. Our analysis further revealed that this 5′ region comprises an intron with at least two different splicing variants. Only one splicing variant results in a continuous open reading frame encoding a deduced amino acid sequence of 485 aa. Based on these sequence analyses, we characterized the identified velvet proteins in detail to decipher their role in *P. chrysogenum*.

Array analyses identify regulatory networks in *P. chrysogenum*. We have recently reported two separate microarray analyses using knockout mutants for PcvelA and PclaeA, as well as the reference Δ*Pcku70* strain for comparison (26). Here we provide a pairwise comparison of two array analyses to investigate the differential transcriptional expression levels in the Δ*PcvelA* and Δ*PclaeA* strains. We first analyzed the expression of genes for velvet subunits and found that the P*cvelC* transcription level is increased in the Δ*PclaeA* strain (see Fig. S4 in the supplemental material). Previously, we have also shown that in this mutant, the level of P*cvosA* transcript is decreased (45), whereas that of P*claeA* is increased in a Δ*PcvelA* mutant (26). We therefore concluded that PcLaeA acts as a positive and negative regulator of P*cvosA* and P*cvelC* transcription, respectively. Moreover, our array analyses revealed that PcVelA is a repressor of P*claeA* transcription. The heat map in Fig. S4 in the supplemental material further shows that genes for putative transcription factors PcWetA, PcAbaA, and PcFlbC as well as proteins most probably involved in the regulation of conidiation (PcPhiA, PcMedA, and PcFlbD) (35) are differentially regulated in the two knockout strains. Similarly, other genes involved in determining conidiospore hydrophobicity (P*cdewA*, P*cdewB*, P*crodA*, and P*crodB*) are downregulated in the Δ*PclaeA* strain, but upregulated in the Δ*PcvelA* strain (see Fig. S4 in the supplemental material). Taken together, these results sup-

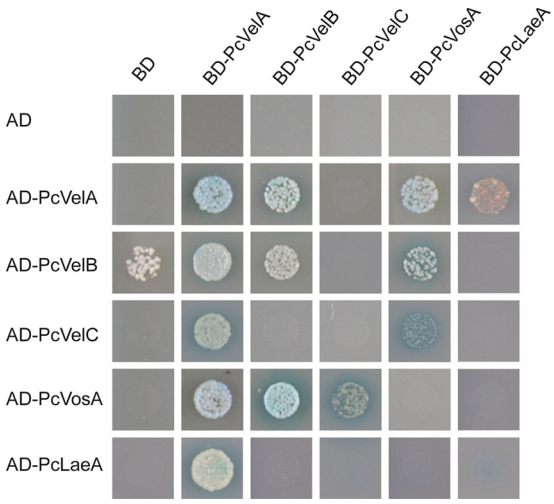

FIG 2 Yeast two-hybrid analysis with components of the velvet complex. Diploid strains synthesizing bait and prey fusion proteins were spotted on selection medium lacking adenine and histidine to show *ADE2* and *HIS3* reporter gene activity. Furthermore, the medium contained X-α-Gal, so that a blue staining of colonies additionally indicates *lacZ* reporter gene activity.

port the view that the velvet complex in *P. chrysogenum* is part of a regulatory network controlling asexual development.

Interaction studies provide evidence of novel subunits in the velvet complex. The microarray analyses demonstrated that components of the velvet complex are part of a regulatory network, and previous interaction studies have provided evidence that a heterotrimeric velvet complex exists in *P. chrysogenum*. The core component of this complex is the velvet homolog PcVelA, which interacts with PcVelB and PcLaeA (26). Since we now had evidence of further velvet proteins (Fig. 1), we investigated direct protein-protein interactions using a yeast two-hybrid assay (Fig. 2). For this purpose, the genes encoding the velvet proteins and PcLaeA were fused with either the Gal4 activation domain or binding domain, and the derived expression vectors were transformed into either AH109 or Y187 from *S. cerevisiae*. The haploid strains were mated and the corresponding diploids were assayed for reporter gene activity by growth on minimal medium lacking histidine and adenine. The medium contains further X-α-Gal to measure expression of the *lacZ* reporter gene, which verifies the protein-protein interaction. Thus, only diploid yeast strains growing on minimal medium and exhibiting blue-colored colonies indicate an interaction between both tested proteins.

As can be seen in Fig. 2, PcVelA, PcVelB, and PcVosA directly interact with each other. The velvet component PcVelC seems to be associated with the complex via PcVosA and possibly also PcVelA. Furthermore, PcLaeA interacts only with PcVelA and not with other velvet components. The yeast two-hybrid results revealed several direct protein-protein interactions between velvet components. However, this method is an *in vitro* approach and might lead to false-positive results. Therefore, we verified the interactions found by yeast two-hybrid analysis through an *in vivo* approach, using bimolecular fluorescence complementation (BiFC) (13). Using this technique, we showed previously that PcVelA interacts with both PcLaeA and PcVelB in the nucleus (26). Here we verify other interactions found by yeast two-hybrid analysis (Fig. 3). In all cases, we found a nuclear localization, which was further confirmed by DAPI staining (Fig. 3A). With this approach, we verified *in vivo* the direct interaction of PcVosA with PcVelA, PcVelB, and PcVelC. Furthermore, the interaction between PcVelA and PcVelC was demonstrated (Fig. 3B).

Taken together, these data indicate that core components like PcVelA and PcVosA might act as bridging factors bringing different velvet components into close proximity and thereby extend

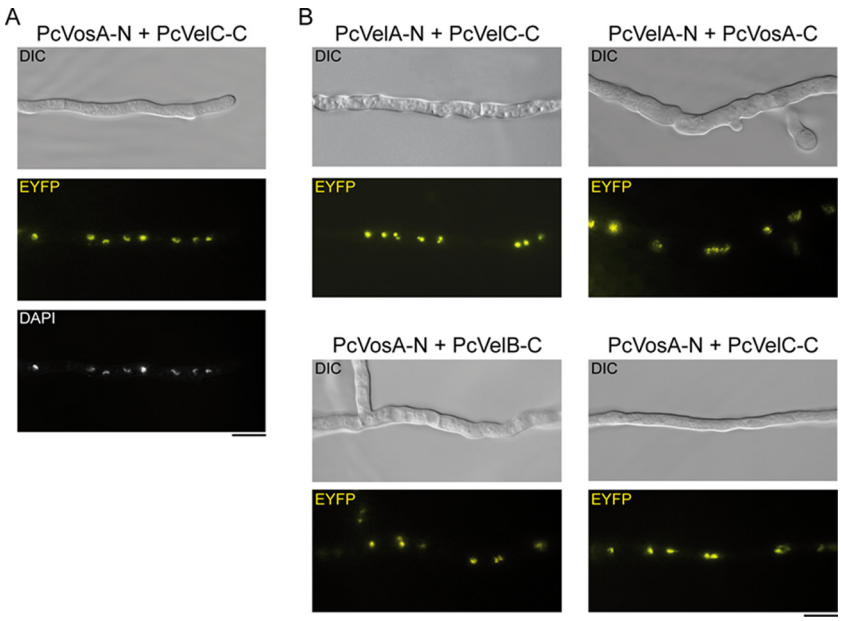

FIG 3 Bimolecular fluorescence complementation studies. (A) Control to confirm the nuclear localization of two interacting velvet components by 4′,6′diamidino-2-phenylindole (DAPI) staining. (B) Protein-protein interactions of components of the velvet protein complex in *P. chrysogenum* as indicated. The fusions of each velvet protein with N- or C-terminal fragments of enhanced yellow fluorescent protein (EYFP) are given above each image set. Micrographs illustrate differential inference contrast (DIC) microscopy, EYFP, or DAPI fluorescence as indicated. Calibration bar, 10 μm.

the current picture of the composition of the velvet complex in *P. chrysogenum* by identifying PcVelB, PcVelC, and PcVosA as new members of the complex, thus providing a basis to better understand the regulatory network controlling morphogenesis and penicillin biosynthesis.

Construction of single and double knockouts for a genetic analysis. Based on our results from the interaction studies, we conducted a functional analysis of components of the velvet complex. For this purpose, we generated single- as well as double-knockout mutants using two different molecular tools recently developed for *P. chrysogenum* (31, 32). As recipient, we used a P*cku70* knockout strain, which is free of any marker gene, generated by the FLP/*FRT* recombination system (32). This strain carries only the 34-bp *FRT* sequence as a remnant of the deleted cassette and allows the successive use of the *nat1* or *ble* resistance marker gene (see Fig. S1 in the supplemental material). As outlined in Materials and Methods, we constructed four knockout strains, the ΔP*cvelA*, ΔP*cvelB*, ΔP*cvelC*, and ΔP*cvosA* strains (see Fig. S2 in the supplemental material). Together with the previously described ΔP*claeA* mutant (26, 33), five mutants lacking single genes for components of the velvet complex were available for our genetic study. Note that our genetic analysis was extended by the construction of four double-knockout strains, using single knockouts as a reference, and the corresponding genealogy of all strains is depicted in Fig. S2 in the supplemental material. This collection of strains, as listed in Table 1, was complemented by the recently described ΔP*claeA* ΔP*cvelA* double mutant (33).

In all experiments, we used two independent single-spore isolates from each knockout strain. As mentioned later, individual knockout strains that had been successfully rescued exhibited the phenotype of the recipient strains, confirming the causal link between mutation and phenotype.

Regulation of penicillin titers through components of the velvet complex. Previously, we have shown that PcVelA and PcLaeA act as positive regulators of penicillin biosynthesis by activating expression of the penicillin biosynthesis genes *pcbAB*, *pcbC*, and *penDE* (26). To further investigate the regulatory role of the newly identified velvet components during penicillin biosynthesis, we used a bioassay with *S. aureus* as a sensitive indicator. To calibrate penicillin activity, the area of the inhibition zone was normalized according to the dry weights, which were measured in parallel from each fungal culture. To confirm that the growth inhibition of *S. aureus* was due to penicillin production, penicillinase was added to the supernatant of selected strains (see Fig. S5 in the supplemental material). In all cases, the addition of penicillinase led to a complete loss of an inhibition zone, thus verifying that the observed halos were a result of penicillin production. It is known from other fungal systems that secondary metabolism is regulated by light (15, 23), and thus the issue arose of whether penicillin production in *P. chrysogenum* is also influenced by light or dark. We performed a penicillin bioassay with the reference strain P2niaD18, grown for 72 h in either light or complete dark. As can be seen in Fig. S6 in the supplemental material, identical penicillin titers can be observed under both conditions, demonstrating that light conditions do not influence penicillin production in this strain. In our initial experiments, penicillin production was tested at four time points (72, 96, 120, and 144 h). As reported previously, an optimal penicillin titer is already obtained after 72 to 96 h (26). However, two of the knockout strains (the ΔP*cvelB* and ΔP*cvosA* strains) showed retarded vegetative growth and reached a maximum mycelium weight and optimal penicillin titer after 144 h. Therefore, for comparison of all tested strains, we determined the values after 144 h of growth in CCM (Fig. 4). Deletion of P*cvelB* resulted in a strain indistinguishable from the recipient ΔP*cku70* strain (Fig. 4). Both strains produced clear halos, thereby confirming proper penicillin titers. Thus, we concluded that PcVelB has no detectable effect on penicillin biosynthesis, a finding that is in contrast to previous results obtained for PcVelA and PcLaeA (26).

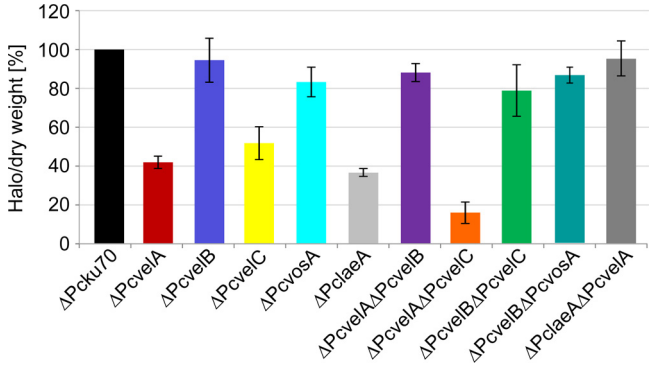

FIG 4 Quantification of penicillin production. Standard deviations were determined from representative isolates, which were measured in triplicate. As a reference, the recently published ΔP*claeA* strain (33) was also measured in triplicate.

Interestingly, we observed that PcVelC has a distinct impact on β-lactam production (Fig. 4). The ΔP*cvelC* strain produced a significantly smaller halo, thereby indicating a marked reduction in penicillin biosynthesis. These results were verified by investigating the corresponding complement ΔP*cvelC*::P*cvelC* strain, showing an inhibition zone similar to that of the recipient ΔP*cku70* strain (data not shown). This result confirms that the lack of the wild-type gene was responsible for the lower penicillin titer. Furthermore, antibiotic activity was severely reduced by about 80% in ΔP*cvelA* ΔP*cvelC* strain (Fig. 4). Compared to the corresponding single knockouts, these findings indicate that PcVelA and PcVelC have an additive effect on penicillin biosynthesis.

Unexpectedly, when we investigated ΔP*cvelA* ΔP*cvelB* and ΔP*cvelB* ΔP*cvelC* double knockouts, our assay values for both double mutants were clearly above those obtained for the ΔP*cvelA* or ΔP*cvelC* strains alone. From this analysis, we conclude that PcVelB represses or inhibits both PcVelA and PcVelC, although in the single PcVelB knockout we did not observe an effect on penicillin titer. Finally, the penicillin activity of the ΔP*claeA* strain was reduced to about 60% after 144 h of cultivation, an observation that corresponds to our previous report (26). We conclude that PcVelA, PcLaeA, and PcVelC seem to activate penicillin biosynthesis, whereas, at least in double mutants, PcVelB appears to play a repressive role in this process.

Impact of velvet components on conidiation. To analyze the impact of velvet components on conidiation, all single- and double-knockout strains were used in phenotypical and quantitative assays (Fig. 5). The drop assay showed reduced conidiospore formation in the ΔP*cvelB* and ΔP*claeA* strains. However, when we investigated double mutants derived from the single knockouts, we found wild-type-like sporulation in some of the derivates. This result indicates that mere additive effects are not responsible for

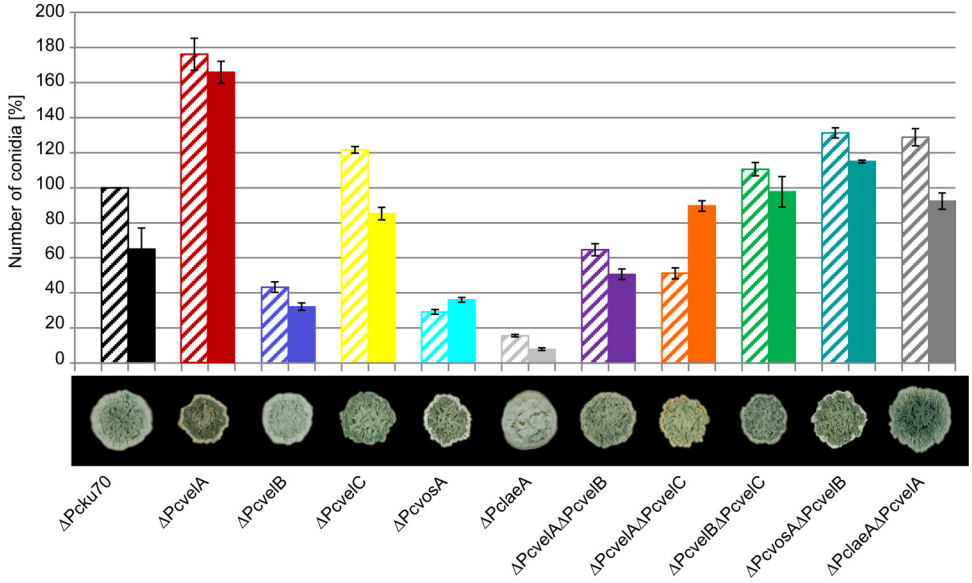

FIG 5 Phenotypic and quantitative conidiation assays. Strains were grown for 7 days on glucose-containing solid minimal medium. Data represent quantification of conidiospore formation under constant light (hatched columns) and dark (solid columns) growth conditions on minimal media with glucose as the sole carbon source. Mean values and standard deviations are derived from the results of three independent experiments. In the bottom row, representative images of colonies are given, showing differences in sporulation rates.

the phenotypes observed. This observation was further specified by our quantitative assay (see below).

On minimal medium with glucose, the reference strain and the ΔPc*velC* strain showed light-dependent conidiation. In the dark, the number of conidiospores declined by about 35%. As reported previously, the ΔPc*velA* strain is not able to sporulate in a light-dependent manner, while the ΔPc*laeA* strain shows a light-independent defect in conidiation (26). Similarly, the ΔPc*velB* strain showed reduced spore formation of about 60%, whereas conidiation significantly increased in the ΔPc*velC* strain. Like the ΔPcvelB strain, the ΔPc*vosA* strain showed a severe conidiation defect with a reduced sporulation of about 70% compared to the ΔPc*ku70* reference strain. Another observation—the formation of light green conidia—resembles the phenotype of the homologous Δ*vosA* mutant from *A. nidulans* (22). The reduced sporulation rate observed for the ΔPc*velB* and ΔPc*vosA* strains prompted us to calculate the spore viability. While the spore viability of the ΔPc*velB* strain was very similar to that of the parental strain (Fig. 6), we found clearly different spore viability in the ΔPc*vosA* mutant, where after 4 days it corresponded to about 20% of that of the reference (ΔPc*ku70*) strain (see Fig. 6). However, measurements after 7, 10, and 13 days showed a clear increase in the spore viability, which finally was close or identical to that of the reference strain.

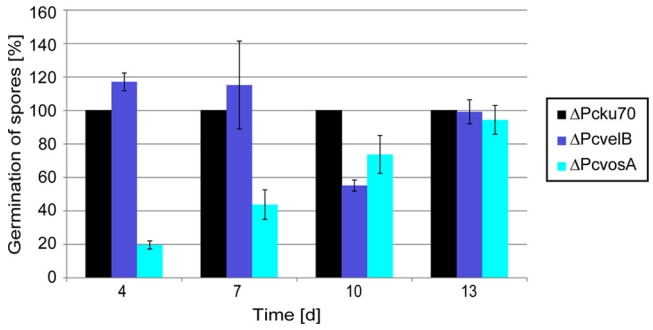

FIG 6 Spore viability assay. For comparison, data from the ΔPc*ku70*, ΔPc*velB*, and ΔPc*vosA* strains are shown.

The quantitative conidiation assay of the double-knockout ΔPc*velB* ΔPc*velC* strain revealed a recipient-like sporulation rate, indicating that PcVelB acts as an activator and PcVelC as a repressor of conidiation. Compared with the two single-knockout mutants, the ΔPc*velA* ΔPc*velB* strain had an intermediate sporulation rate, probably due to the lack of the activator PcVelB. In contrast to the ΔPc*velA* and ΔPc*velC* strains, which both displayed an increased level of conidiation, the corresponding double knockout had a significantly lower sporulation rate. A rather unexpected result was found for the ΔPc*laeA* ΔPc*velA* and ΔPc*velB* ΔPc*vosA* strains, which both formed more spores than the recipient and thus had sporulation rates that were clearly different from those of the two corresponding single knockouts. Interestingly, the corresponding ΔPc*laeA* ΔPc*velA* double mutant from *A. nidulans* was reported to exhibit a similar increase in conidiation on solid media, while the single *laeA* knockout strain was also impaired in conidiation (23). Thus, although spore formation is mediated via PcLaeA, which is negatively controlled upstream by PcVelA (26), the lack of both proteins in the double mutant suggests that conidiation is further regulated by another component(s), for example, PcVelB or PcVosA.

Another feature of some knockout strains was also striking. In detail, it is generally accepted that light signaling is mediated via the Velvet protein (17, 26) (see also ΔPc*velA* strain data in Fig. 5), an assumption that was confirmed by the phenotype of the ΔPc*velA* ΔPc*velB* and ΔPc*velA* ΔPc*velC* strains. However, light regulation is also diminished in the ΔPc*velB* and ΔPc*velB* ΔPc*velC* strains as well as in the single-knockout ΔPc*vosA* strain and in the

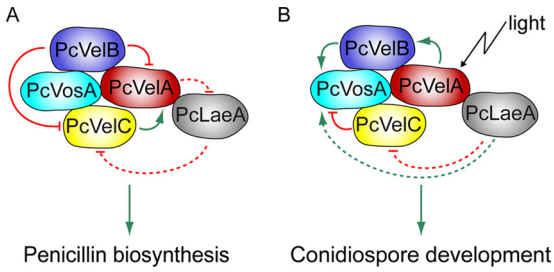

FIG 7 Working model for the function of the velvet complex in *P. chrysogenum*. Depicted functional subcomplexes with different subunit compositions differentially control penicillin biosynthesis (A) and conidiospore development (B). The green or red arrows indicate whether single subunits seem to possess an activating or a repressing function, respectively. The dotted and solid lines represent conclusions drawn from microarray and mutant analyses, respectively.

corresponding ΔPc*velB* ΔPc*vosA* double mutant, thus indicating that PcVelB and PcVosA are also involved in light signaling.

In addition, the unexpected phenotype of the ΔPc*laeA* ΔPc*velA* strain with wild-type-like light-dependent conidiation even suggests that in the double mutant, PcVelB is able to compensate for the missing light signaling of PcVelA. Our quantitative assays provide evidence that conidiation is controlled by opposing effects of PcVelB and PcVelC and further suggest an involvement of PcVelB and PcVosA in light signaling.

DISCUSSION

Velvet proteins play opposing roles during penicillin biosynthesis. Penicillin biosynthesis and conidiospore development in *Penicillium chrysogenum* are controlled by components of the multisubunit velvet complex (see Fig. 7). Previously, we identified PcVelA and PcLaeA (26) and describe here further subunits as new members of this complex. While homologs of PcVosA and PcVelB have been described for other filamentous fungi (17, 22, 23, 47, 48), we provide the first functional characterization for a VelC homolog.

For example, our study provides strong evidence that PcvelC interacts with other components of the velvet complex and that PcVelC acts as a strong activator of penicillin production and therefore controls secondary metabolite production together with PcVelA and PcLaeA in *P. chrysogenum*. Since deletion of both activators, PcVelC and PcVelA, leads to an additive effect in the reduction of penicillin biosynthesis, we propose that penicillin biosynthesis is regulated synergistically by PcVelA and PcVelC. Most interestingly, we found that penicillin biosynthesis is controlled by the opposing effects of PcVelB and PcVelC. Moreover, functional characterization of single- and double-knockout mutants led us conclude that PcVelB acts as a repressor of PcVelA and PcVelC since the ΔPc*velA* ΔPc*velB* and ΔPc*velB* ΔPc*velC* strains clearly show a higher rate of penicillin biosynthesis than the ΔPc*velA* and ΔPc*velC* single mutants. However, we did not observe an increase in penicillin titer in the ΔPc*velB* mutant, an observation that might be explained by the fact that the reference strain had already reached the upper limit of penicillin production and, thus, that a further increase in production was highly unlikely to obtain. Interestingly, the observed function of PcVelB is distinct from those of its homologs in both *A. nidulans* and *Fusarium fujikuroi*. In those two fungi, the corresponding deletion strains are impaired in secondary metabolism, thereby indicating an activating role for VelB (17, 48).

PcVelB and PcVosA activate conidiation whereas PcVelC represses conidiation. The knockout analysis shows that conidiation is significantly reduced in the ΔPc*velB* strain whereas, in the ΔPc*velC* strain, spore formation is increased. However, in the corresponding ΔPc*velB* ΔPc*velC* double mutant, conidiospore formation seems to be similar to that of the recipient, indicating that PcVelB and PcVelC play opposite roles during asexual development. We therefore propose that PcVelB acts as an activator and PcVelC as a repressor of conidiospore formation—the complete reverse of their functional roles in penicillin biosynthesis. VelB homologs are already known to have an activating role in regulating conidiation. In *F. fujikuroi*, deletion of *Ffvel2* resulted in reduced formation of microconidia, while in *Histoplasma capsulatum*, Ryp3 is required together with the VosA homolog Ryp2 to produce normal viable spores in a temperature-dependent manner (47, 48).

Data from this as well as other studies (23) support the notion that PcLaeA is connected with PcVelA and thus is part of the velvet complex (Fig. 7B). There is evidence that PcLaeA acts as a regulator of asexual spore formation, since the ΔPc*laeA* mutant shows a drastic reduction of spore formation (26). These data might be explained by the fact that PcLaeA stimulates conidiation by regulation of gene expression. In *P. chrysogenum*, deletion of Pc*laeA* led to an increase of Pc*velC* transcripts, resulting most likely in an increased amount of the repressor protein. Furthermore, a decrease of Pc*vosA* expression was observed in another array analysis (45), suggesting that proper signaling through this protein might be disturbed. PcLaeA is known to be negatively controlled upstream by PcVelA (26); thus, deletion of both proteins seems to mediate conidiation to a downstream component, most probably PcVosA, in an unimpeded manner. Furthermore, our microarray data revealed that *abaA* and *wetA* are two of several genes negatively controlled by PcLaeA, and comparable data showing transcript levels for *abaA* were reported for *A. nidulans* (23). AbaA is a well-conserved transcription factor which, together with BrlA and WetA, forms a central regulatory pathway that controls asexual spore formation (49). Thus, downregulation of both genes might result in a severe impairment in conidiation.

The defect observed for the *P. chrysogenum* ΔPc*laeA* mutant resembles the phenotype of the corresponding mutant from *A. nidulans*, where LaeA is also required to allow asexual development in light. In both *P. chrysogenum* and *A. nidulans*, double-knockout mutants lacking genes for the LaeA and VeA subunits show an increased conidiation on solid media, although the LaeA knockout strain is impaired in conidiation. Recently, it was suggested that LaeA seems to be functional only when it interacts with an intact VeA polypeptide and that it controls asexual formation in an as-yet-unknown manner (23).

Our quantification assay revealed light-dependent conidiospore formation in *P. chrysogenum*. Previous studies have already shown that deletion of Pc*velA* results in the production of an almost equal number of conidia that are independent of light, indicating that light signaling is mediated via PcVelA (26). This assumption is further confirmed by the observed blind phenotype of the ΔPc*velA* ΔPc*velB* and ΔPc*velA* ΔPc*velC* strains, and our data are consistent with results obtained from other filamentous fungi where proper expression of *velvet* is necessary for asexual conidial formation (19).

Previously, VeA from *A. nidulans* was suggested to be regulated through the phosphorylation status of the protein (18). It can thus be speculated that transphosphorylation of VeA leads to activation of downstream components and thus to induction of the asexual pathway in light. Furthermore, VelB is also known to be a light-dependent regulator of conidiation (17). For example, this protein interacts with VosA only in the dark to repress asexual development, while light inhibits the formation of this subcomplex. Our results are consistent with these data. PcVelB is also involved in light signaling, providing evidence for the presence of a similar regulatory network in *P. chrysogenum*. In the ΔPc*velB* and ΔPc*velB* ΔPc*velC* strains, we found that light regulation is diminished and that the phenotype of the ΔPc*laeA* ΔPc*velA* strain includes light-dependent conidiation comparable to that seen with the wild type, thereby suggesting that PcVelB or another velvet component can compensate for the missing light signaling of PcVelA (Fig. 7B). Furthermore, loss of light-dependent conidiation in the ΔPc*velB* ΔPc*velC* and ΔPc*velB* ΔPc*vosA* strains, despite the presence of PcVelA in these mutants, suggests that light perception is transmitted from PcVelA to other velvet components. Finally, our data indicate that PcVelC is not involved in light signaling, since the corresponding mutant responds like the wild type to light.

For *A. nidulans*, the levels of VelB and VosA were reduced during the light response by LaeA, and thus, the VelB-VosA heterodimer is hardly detectable. The low level of this heterodimer abolishes the repression of asexual development that takes place during growth in the dark. Without LaeA, protein levels of VelB and VosA are significantly elevated, resulting in an increased repression of conidiation (23).

Working model. Our genetic analysis provides evidence for a regulatory link between penicillin biosynthesis and conidiation. As depicted in our model (Fig. 7), we propose a velvet complex in *P. chrysogenum* in which components affect each other differently during secondary metabolism and conidiospore development. Our interaction studies demonstrate that all velvet subunits can interact with one or more other subunits. However, whether subcomplexes are formed at distinct time points or developmental stages is an interesting but still open issue. It was already shown for *A. nidulans* that velvet components form subcomplexes with different functions (23). It remains an interesting task for further studies to determine whether similar subcomplexes can be identified in *P. chrysogenum* or other filamentous ascomycetes.

The distinct interplay of subunits of the velvet complex is supported by our array data that show decreased transcript levels of Pc*vosA* but increased levels of Pc*velC* in the ΔPc*laeA* mutant. These results suggest that PcLaeA, as a member of the complex, plays a regulatory role in *P. chrysogenum*. Moreover, deletion of Pc*velA* positively affects Pc*laeA* transcript levels, while the loss of Pc*laeA* increases Pc*velC* gene expression. Similarly, protein complexes containing interacting factors having opposing roles were previously identified in other fungi, where VeA and LaeA have opposite functions in light control (23, 48). In detail, whereas in the *veA*Δ mutant, the asexual program is constitutive when LaeA is present, the *laeA*Δ mutant almost exclusively forms cleistothecia and the number of asexual spores are drastically reduced (23).

A new finding of this study is the opposing regulatory roles played by PcVelB and PcVelC in the velvet complex in *P. chrysogenum*. An alternative counteracting role of proteins was described for several transcription factors. In *A. nidulans*, the well-conserved tetrameric HapB-HapC-HapE-HapX complex, designated AnCF, links the regulation of secondary metabolite production and asexual fungal development (50). The complex binds to the CCAAT motif in the promoter of penicillin biosynthesis genes and is essential for the expression of penicillin (51). However, the basic-region helix-loop-helix transcription factor AnBH1 counteracts the positive action of AnCF (52). In the dimorphic yeast *Candida albicans*, genetic analysis of single- and double-deletion mutants showed that the transcription factors SflI and Flo8 play opposing roles in the regulation of filamentous growth in liquid and solid media (53). For higher eukaryotes, several other examples have also been described. In *Arabidopsis thaliana*, gene expression of *DEL1*, a negative regulator of the endocycle (onset), is antagonistically controlled by the transcription factors E2Fb and E2Fc, which compete for a single E2F *cis*-acting binding site (54). Similarly, in *Nicotiana tabacum*, the expression level of the invertase gene *NIN88*, a core protein of pollen development, is regulated by counteracting homo- and heterodimers of bZIP transcription factors BZI-1, BZI-2, and BZI-4 (55). The above-mentioned opposing roles of transcription factors are in line with a recent assumption that suggested a function of velvet components as transcription factors controlling fungus-specific developmental processes (22). Future research on velvet complexes in diverse fungal systems will likely provide further evidence for their predicted function and thus promote our understanding of the mechanistic role of these complexes. Such studies will be relevant for the genetic manipulation of fungal metabolism as part of industrial strain improvement programs.

ACKNOWLEDGMENTS

We are grateful to Stefanie Mertens, Ivonne Schelberg, Kerstin Kalkreuter, Ingeborg Godehardt, and Susanne Schlewinski for their excellent technical assistance, Gabriele Frenßen-Schenkel for the artwork, and Hubert Kürnsteiner, Ivo Zadra, Ernst Friedlin, Rudolf Mitterbauer, and Thomas Specht (Sandoz GmbH, Kundl, Austria) for fruitful discussions. We thank Sarah Milbredt and Janina Kluge for their help with some of the experiments, as well as Tim Dahlmann and Simon Wolfers for help with bioinformatic data.

This work was funded by the Christian Doppler Society (Vienna, Austria) and by Sandoz GmbH (Kundl, Austria).

REFERENCES

1. **Fleming A.** 1929. On the antibacterial action of cultures of a *Penicillium*, with special reference to their use in the isolation of *B. influenzae*. Br. J. Exp. Pathol. **10**:226–236.
2. **Barber MS, Giesecke U, Reichert A, Minas W.** 2004. Industrial enzymatic production of cephalosporin-based beta-lactams. Adv. Biochem. Eng. Biotechnol. **88**:179–215.
3. **van den Berg MA.** 2011. Impact of the *Penicillium chrysogenum* genome on industrial production of metabolites. Appl. Microbiol. Biotechnol. **92**: 45–53.
4. **Brakhage AA, Spröte P, Al-Abdallah Q, Gehrke A, Plattner H, Tüncher A.** 2004. Regulation of penicillin biosynthesis in filamentous fungi. Adv. Biochem. Eng. Biotechnol. **88**:45–90.
5. **Martín JF, Liras P.** 1989. Organization and expression of genes involved in the biosynthesis of antibiotics and other secondary metabolites. Annu. Rev. Microbiol. **43**:173–206.
6. **Woloshuk CP, Prieto R.** 1998. Genetic organization and function of the aflatoxin B1 biosynthetic genes. FEMS Microbiol. Lett. **160**:169–176.
7. **Yu JH, Keller N.** 2005. Regulation of secondary metabolism in filamentous fungi. Annu. Rev. Phytopathol. **43**:437–458.
8. **Calvo AM, Wilson RA, Bok JW, Keller NP.** 2002. Relationship between secondary metabolism and fungal development. Microbiol. Mol. Biol. Rev. **66**:447–459.
9. **Tag A, Hicks J, Garifullina G, Ake C, Phillips TD, Beremand M, Keller**

N. 2000. G-protein signalling mediates differential production of toxic secondary metabolites. Mol. Microbiol. **38**:658–665.
10. **Hicks JK, Yu JH, Keller NP, Adams TH.** 1997. *Aspergillus* sporulation and mycotoxin production both require inactivation of the FadA G alpha protein-dependent signaling pathway. EMBO J. **16**:4916–4923.
11. **Keller NP, Turner G, Bennett JW.** 2005. Fungal secondary metabolism—from biochemistry to genomics. Nat. Rev. Microbiol. **3**:937–947.
12. **Schmitt EK, Hoff B, Kück U.** 2004. AcFKH1, a novel member of the forkhead family, associates with RFX transcription factor CPCR1 in the cephalosporin C-producing fungus *Acremonium chrysogenum*. Gene **342**: 269–281.
13. **Hoff B, Kück U.** 2005. Use of bimolecular fluorescence complementation to demonstrate transcription factor interaction in nuclei of living cells from the filamentous fungus *Acremonium chrysogenum*. Curr. Genet. **47**: 132–138.
14. **Hoff B, Schmitt EK, Kück U.** 2005. CPCR1, but not its interacting transcription factor AcFKH1, controls fungal arthrospore formation in *Acremonium chrysogenum*. Mol. Microbiol. **56**:1220–1233.
15. **Kato N, Brooks W, Calvo AM.** 2003. The expression of sterigmatocystin and penicillin genes in *Aspergillus nidulans* is controlled by *veA*, a gene required for sexual development. Eukaryot. Cell **2**:1178–1186.
16. **Spröte P, Brakhage AA.** 2007. The light-dependent regulator velvet A of *Aspergillus nidulans* acts as a repressor of the penicillin biosynthesis. Arch. Microbiol. **188**:69–79.
17. **Bayram Ö, Krappmann S, Ni M, Bok JW, Helmstaedt K, Valerius O, Braus-Stromeyer S, Kwon NJ, Keller NP, Yu JH, Braus GH.** 2008. VelB/VeA/LaeA complex coordinates light signal with fungal development and secondary metabolism. Science **320**:1504–1506.
18. **Purschwitz J, Müller S, Fischer R.** 2009. Mapping the interaction sites of *Aspergillus nidulans* phytochrome FphA with the global regulator VeA and the White Collar protein LreB. Mol. Genet. Genomics **281**:35–42.
19. **Calvo AM.** 2008. The VeA regulatory system and its role in morphological and chemical development in fungi. Fungal Genet. Biol. **45**:1053–1061.
20. **Käfer E.** 1965. Origins of translocations in *Aspergillus nidulans*. Genetics **52**:217–232.
21. **Bok JW, Keller NP.** 2004. LaeA, a regulator of secondary metabolism in *Aspergillus* spp. Eukaryot. Cell **3**:527–535.
22. **Ni M, Yu JH.** 2007. A novel regulator couples sporogenesis and trehalose biogenesis in *Aspergillus nidulans*. PLoS One **2**:e970. doi:10.1371/journal.pone.0000970.
23. **Sarikaya Bayram Ö, Valerius O, Park HS, Irniger S, Gerke J, Ni M, Han KH, Yu JH, Braus GH.** 2010. LaeA control of velvet family regulatory proteins for light-dependent development and fungal cell-type specificity. PLoS Genet. **6**:e1001226. doi:10.1371/journal.pgen.1001226.
24. **Bayram Ö, Braus GH.** 2012. Coordination of secondary metabolism and development in fungi: the velvet family of regulatory proteins. FEMS Microbiol. Rev. **36**:1–24.
25. **Myung K, Zitomer NC, Duvall M, Glenn AE, Riley RT, Calvo AM.** 2012. The conserved global regulator VeA is necessary for symptom production and mycotoxin synthesis in maize seedlings by *Fusarium verticillioides*. Plant Pathol. **61**:152–160.
26. **Hoff B, Kamerewerd J, Sigl C, Mitterbauer R, Zadra I, Kürnsteiner H, Kück U.** 2010. Two components of a velvet-like complex control hyphal morphogenesis, conidiophore development, and penicillin biosynthesis in *Penicillium chrysogenum*. Eukaryot. Cell **9**:1236–1250.
27. **Sambrook J, Russell DW.** 2001. Molecular cloning, a laboratory manual, 3rd ed. Cold Spring Harbor Laboratory Press, Cold Spring Habor, NY.
28. **Bullock WO, Fernandez JM, Short JM.** 1987. XL1-Blue: a high efficiency plasmid transforming *recA Escherichia coli* strain with β-galactosidase selection. Biotechniques **5**:376–378.
29. **Colot HV, Park G, Turner GE, Ringelberg C, Crew CM, Litvinkova L, Weiss RL, Borkovich KA, Dunlap JC.** 2006. A high-throughput gene knockout procedure for *Neurospora* reveals functions for multiple transcription factors. Proc. Natl. Acad. Sci. U. S. A. **103**:10352–10357.
30. **Becker DM, Lundblad V.** 1994. Introduction of DNA into yeast cells, p 13.17.11-13.17.10. *In* Ausubel FM, Brent R, Kingston RE, Moore DD, Seidmann JG, Smith JA, Struhl K (ed), Current protocols in molecular biology. John Wiley & Sons, Inc., Hoboken, NJ.
31. **Hoff B, Kamerewerd J, Sigl C, Zadra I, Kück U.** 2010. Homologous recombination in the antibiotic producer *Penicillium chrysogenum*: strain ΔPcku70 shows up-regulation of genes from the HOG pathway. Appl. Microbiol. Biotechnol. **85**:1081–1094.
32. **Kopke K, Hoff B, Kück U.** 2010. Application of the *Saccharomyces cerevisiae* FLP/*FRT* recombination system in filamentous fungi for marker recycling and construction of knockout strains devoid of heterologous genes. Appl. Environ. Microbiol. **76**:4664–4674.
33. **Janus D, Hoff B, Kück U.** 2009. Evidence for Dicer-dependent RNA interference in the industrial penicillin producer *Penicillium chrysogenum*. Microbiology **155**:3946–3956.
34. **Hoff B, Pöggeler S, Kück U.** 2008. Eighty years after its discovery, Fleming's *Penicillium* strain discloses the secret of its sex. Eukaryot. Cell **7**:465–470.
35. **van den Berg MA, Albang R, Albermann K, Badger JH, Daran JM, Driessen AJ, Garcia-Estrada C, Fedorova ND, Harris DM, Heijne WH, Joardar V, Kiel JA, Kovalchuk A, Martín JF, Nierman WC, Nijland JG, Pronk JT, Roubos JA, van der Klei IJ, van Peij NN, Veenhuis M, von Döhren H, Wagner C, Wortman J, Bovenberg RA.** 2008. Genome sequencing and analysis of the filamentous fungus *Penicillium chrysogenum*. Nat. Biotechnol. **26**:1161–1168.
36. **Zadra I, Abt B, Parson W, Haas H.** 2000. *xylP* promoter-based expression system and its use for antisense downregulation of the *Penicillium chrysogenum* nitrogen regulator NRE. Appl. Environ. Microbiol. **66**:4810–4816.
37. **Christianson TW, Sikorski RS, Dante M, Shero JH, Hieter P.** 1992. Multifunctional yeast high-copy-number shuttle vectors. Gene **110**:119–122.
38. **Jekosch K, Kück U.** 2000. Loss of glucose repression in an *Acremonium chrysogenum* beta-lactam producer strain and its restoration by multiple copies of the *cre1* gene. Appl. Microbiol. Biotechnol. **54**:556–563.
39. **Schmitt EK, Bunse A, Janus D, Hoff B, Friedlin E, Kürnsteiner H, Kück U.** 2004. Winged helix transcription factor CPCR1 is involved in regulation of beta-lactam biosynthesis in the fungus *Acremonium chrysogenum*. Eukaryot. Cell **3**:121–134.
40. **Bloemendal S, Bernhards Y, Bartho K, Dettmann A, Voigt O, Teichert I, Seiler S, Wolters DA, Pöggeler S, Kück U.** 2012. A homologue of the human STRIPAK complex controls sexual development in fungi. Mol. Microbiol. **84**:310–323.
41. **Horton P, Park KJ, Obayashi T, Fujita N, Harada H, Adams-Collier CJ, Nakai K.** 2007. WoLF PSORT: protein localization predictor. Nucleic Acids Res. **35**:W585–W587.
42. **la Cour T, Kiemer L, Molgaard A, Gupta R, Skriver K, Brunak S.** 2004. Analysis and prediction of leucine-rich nuclear export signals. Protein Eng. Des. Sel. **17**:527–536.
43. **Thompson JD, Higgins DG, Gibson TJ.** 1994. CLUSTAL W: improving the sensitivity of progressive multiple sequence alignment through sequence weighting, position-specific gap penalties and weight matrix choice. Nucleic Acids Res. **22**:4673–4680.
44. **Nicholas KB, Nicholas HB, Deerfield DW, II.** 1997. GeneDoc: analysis and visualization of genetic variation. EMBNEW.News **4**:14.
45. **Kamerewerd J, Zadra I, Kürnsteiner H, Kück U.** 2011. *PcchiBI*, encoding a class V chitinase, is affected by PcVelA and PcLaeA and responsible for cell wall integrity in *Penicillium chrysogenum*. Microbiology **157**:3036–3048.
46. **Stinnett SM, Espeso EA, Cobeno L, Araújo-Bazán L, Calvo AM.** 2007. *Aspergillus nidulans* VeA subcellular localization is dependent on the importin α carrier and on light. Mol. Microbiol. **63**:242–255.
47. **Webster RH, Sil A.** 2008. Conserved factors Ryp2 and Ryp3 control cell morphology and infectious spore formation in the fungal pathogen *Histoplasma capsulatum*. Proc. Natl. Acad. Sci. U. S. A. **105**:14573–14578.
48. **Wiemann P, Brown DW, Kleigrewe K, Bok JW, Keller NP, Humpf HU, Tudzynski B.** 2010. FfVel1 and FfLae1, components of a *velvet*-like complex in *Fusarium fujikuroi*, affect differentiation, secondary metabolism and virulence. Mol. Microbiol. **77**:972–994.
49. **Andrianopoulos A, Timberlake WE.** 1994. The *Aspergillus nidulans abaA* gene encodes a transcriptional activator that acts as a genetic switch to control development. Mol. Cell. Biol. **14**:2503–2515.
50. **Hortschansky P, Eisendle M, Al-Abdallah Q, Schmidt AD, Bergmann S, Thon M, Kniemeyer O, Abt B, Seeber B, Werner ER, Kato M, Brakhage AA, Haas H.** 2007. Interaction of HapX with the CCAAT-binding complex—a novel mechanism of gene regulation by iron. EMBO J. **26**:3157–3168.
51. **Steidl S, Papagiannopoulos P, Litzka O, Andrianopoulos A, Davis MA, Brakhage AA, Hynes MJ.** 1999. AnCF, the CCAAT binding complex of *Aspergillus nidulans*, contains products of the *hapB*, *hapC*, and *hapE* genes and is required for activation by the pathway-specific regulatory gene *amdR*. Mol. Cell. Biol. **19**:99–106.
52. **Caruso ML, Litzka O, Martic G, Lottspeich F, Brakhage AA.** 2002. Novel

basic-region helix-loop-helix transcription factor (AnBH1) of *Aspergillus nidulans* counteracts the CCAAT-binding complex AnCF in the promoter of a penicillin biosynthesis gene. J. Mol. Biol. **323**:425–439.
53. **Li Y, Su C, Mao X, Cao F, Chen J.** 2007. Roles of Candida albicans Sfl1 in hyphal development. Eukaryot. Cell **6**:2112–2121.
54. **Berckmans B, Lammens T, Van Den Daele H, Magyar Z, Bogre L, De Veylder L.** 2011. Light-dependent regulation of DEL1 is determined by the antagonistic action of E2Fb and E2Fc. Plant Physiol. **157**:1440–1451.
55. **Iven T, Strathmann A, Bottner S, Zwafink T, Heinekamp T, Guivarc'h A, Roitsch T, Droge-Laser W.** 2010. Homo- and heterodimers of tobacco bZIP proteins counteract as positive or negative regulators of transcription during pollen development. Plant J. **63**:155–166.